Journal of Physical Science, Vol. 35(3), 1–15, 2024

TiO_2/Polysulfone Composite Membrane for Enhanced Removal of Acetaminophen from Water

Wan Khairunnisa Wan Ramli,* Norakma Dollah and Oon Li Qing

Faculty of Chemical Engineering & Technology, Kompleks Pusat Pengajian Jejawi 3, Universiti Malaysia Perlis, 02600 Arau, Perlis, Malaysia

*Corresponding author: wankhairunnisa@unimap.edu.my

Published online: 30 November 2024

To cite this article: Ramli, W. K. W., Dollah, N. & Onn, L. Q. (2024). TiO_2/polysulfone composite membrane for enhanced removal of acetaminophen from water. *J. Phys. Sci.*, 35(3), 1–15. https://doi.org/10.21315/jps2024.35.3.1

To link this article: https://doi.org/10.21315/jps2024.35.3.1

ABSTRACT: *There has been a significant rise in the worldwide usage of acetaminophen (ACT), particularly after the COVID-19 pandemic, leading to concerns regarding its possible discharge into the environment. Even at low levels, the gradual buildup of ACT can present a significant risk to both aquatic ecosystems and human health, especially when consumed through drinking water. The advanced oxidation process (AOP) is an excellent treatment technique for removing ACT. However, it is a complex and expensive procedure that consumes a significant amount of energy. Membrane technology has evolved as a viable and efficient method to eliminate ACT, offering a simpler and more energy-efficient approach. This study examined the impact of different concentrations of titanium dioxide (TiO_2) nanofiller on the elimination of ACT from a water-based solution. The membrane containing the highest concentration of TiO_2 (2 wt.%) demonstrated the greatest water flux and ACT removal rate at 32 L/m^{2}h and 97%, respectively. The inclusion of TiO_2 had a substantial impact on the structure of the membrane, leading to the formation of evenly distributed finger-like pores throughout a spongy framework. This modification resulted in enhanced flow rate and increased efficiency in terms of the flux and rejection rate.*

Keywords: Polysulfone, titanium dioxide, acetaminophen removal, membrane separation, nanofiller

© Penerbit Universiti Sains Malaysia, 2024. This work is licensed under the terms of the Creative Commons Attribution (CC BY) (http://creativecommons.org/licenses/by/4.0/).

1. INTRODUCTION

Drinking waters, other water reserves and the effluents of sewage treatment plants (STPs) are frequently found to contain pharmaceutical active compounds (PhACs). This is primarily because new chemical compounds are being used more frequently as a result of medical technology advancements. These compounds can have negative effects on the environment and public health even at low concentrations, which leads to the discovery of new micropollutant traces in the water environment. The release of these intricately structured and chemically complex micropollutants into water requires the development of increasingly sophisticated and effective methods to address the problem.

Acetaminophen (ACT), commonly referred to as paracetamol is a widely used painkiller that is available over the counter without a prescription. Due to its widespread use across the globe, ACT may be released into the environment through several means, including animal and human excretion, inappropriate drug disposal and wastewater treatment plant effluents. Because of this, trace amounts of ACT have been found in drinking water sources, groundwater and surface water across the globe. According to Shipingana et al., 4.6 μg/ml of ACT was detected at the inlet of a municipal wastewater treatment in Mysuru City, India.[1] Its presence in water bodies may affect aquatic organisms ecologically. Even though the concentrations of ACT in water sources are typically low and unlikely to pose a direct risk to human health through drinking water consumption, there is growing concern about the potential accumulation of these PhACs over time in the environment and their long-term effects on ecosystems and human health.

Advanced oxidation processes (AOPs), adsorption and membrane technology are examples of novel treatment techniques that have improved wastewater treatments at present, particularly in the removal of these micropollutants.[2] In the case of AOP, this entails the production and application of an oxidant; the hydroxyl radical through several intricate processes, including ozonation and photolysis. The method removed PhACs with high efficacy, but it exhibited significant flaws, particularly concerning cost, energy consumption and process complexity. Membrane technology shows superior advantages over other technologies with similar separation efficiency since it is more cost-effective, involves a simpler setup and ecologically friendly. Membranes are commonly made of polymer and ceramic materials, and polymeric membranes are the most popular due to their higher selectivity and can be easily functionalised or modified to suit specific pollutants.

Polysulfone (PSf) is extensively utilised as an efficient membrane material owing to its ability to synthesise polymeric membranes for various applications via simpler methods such as phase inversion, but its inherent hydrophobicity restricts its application in water separation.[3,4] Various studies have been performed to enhance its hydrophilicity including the usage of complicated synthesis method such as chemical grafting and plasma modification. The incorporation of additives, specifically adsorptive and hydrophilic particles, such as activated carbon, Al_2O_3, SiO_2 and TiO_2 by polymer/additive blending has shown potential in improving the membrane structure and effectively removing toxic particulates such as ACT. Nadour et al. demonstrated that the addition of methylcellulose and activated carbon as adsorptive particles into the PSf membrane can significantly improve surface hydrophilicity and membrane rigidity, subsequently enhancing the water permeability and increasing ACT removal.[5] TiO_2 in particular, have also attracted augmented interest due to their good chemical stability, elevated hydrophilicity and antibacterial properties.[6] Zhang et al. reported that the addition of TiO_2 sol in the PSf blend significantly improves the overall properties of the membrane especially in terms of porosity, hydrophilicity and anti-fouling.[7] Several other works also reported on the enhanced hydrophilicity and other properties such as membrane morphology of PSf and polyethersulfone (PES) membranes after the addition of TiO_2.[8,9]

This work aims to evaluate the influence of varying TiO_2 concentrations in the PSf membrane matrix on the membrane characteristics and the removal of ACT. In our knowledge, no study was done to evaluate the effect of TiO_2 addition into PSf membrane to remove ACT. Lower concentrations of TiO_2 in the range of 0 wt.%–2 wt.% were chosen for this preliminary study since it has been reported previously that the addition of higher concentrations of TiO_2 (> 2 wt.%) could result in severe particle aggregation, subsequently reducing the efficiency of the membrane.[6,10] The membranes were prepared via the simple immersion precipitation method. The performance of the membranes was evaluated to remove ACT from aqueous solution and was compared to those obtained by membrane without TiO_2.

2. EXPERIMENTAL

2.1 Materials

Polysulfone (PSf, Udel® P-1700, MW = 67,000 g/mol) was acquired from Solvay Solexis, France. Titanium Dioxide (TiO_2, Degussa P25) was purchased from Merck. N-methyl-2-pyrrolidone (NMP, ≥ 99.5%) and ACT were obtained from Sigma Aldrich. Deionised (DI) water was used as the coagulant. Liquid and

gaseous nitrogen (N_2) were provided by Bann Edar, Malaysia. The PSf and TiO_2 powders were dried overnight at 100°C in an oven before use. Other chemicals were used as received.

2.2 TiO_2/PSf Membranes Synthesis

TiO_2/PSf membranes were prepared via the immersion precipitation method and the dope solutions were prepared following the methods from Ramli et al.[11] Various concentrations of TiO_2 NPs (0.5 wt.%–2.0 wt.%), as shown in Table 1, were dissolved in NMP at 60°C and stirred at 300 rpm. Subsequently, PSf was added gradually to the mixture under continuous stirring for 6 h or until all the powder dissolved. The solution was degassed, cooled and cast using a casting machine with a pre-set casting thickness of 250 μm. The casted film was rapidly immersed in a coagulation bath containing DI water for 24 h. The synthesised membranes were then washed and dried.

Table 1: Compositions of the synthesised membranes.

Membrane	PSf (wt.%)	TiO_2 (wt.%)	NMP (wt.%)
Ti-0.0	17	–	83.0
Ti-0.5	17	0.5	82.5
Ti-1.0	17	1.0	82.0
Ti-1.5	17	1.5	81.5
Ti-2.0	17	2.0	81.0

2.3 Membrane Characterisations

The surface and cross-sectional morphologies of the membranes (1 cm × 1 cm) were examined under the scanning electron microscope (SEM; JEOL, JSM-6460LA) at an accelerating voltage of 15 kV. For the cross-sectional images, the synthesised membranes were fractured in liquid N_2 and coated with platinum. The fourier transform infrared (FTIR) spectra of the membranes were established using an FTIR Spectrophotometer (Perkin Elmer) in the region of 650 cm^{-1}–4,000 cm^{-1} to confirm the addition of TiO_2 into the PSf backbone. The membrane was immersed in DI water for 2 h to measure the membrane's porosity. Before determining the weight of the wet membrane, w_w, the membrane was gently patted to remove any remaining liquid from the surface. The membrane was then dried in an oven for 48 h to make sure it was completely dry before measuring the weight of the dried membrane, w_d. The membrane was weighed periodically until the weights were constant. The membrane porosity, ε can be calculated using Equation 1:[12]

$$\varepsilon = \frac{\frac{(w_w - w_d)}{\rho_e}}{\frac{(w_w - w_d)}{\rho_e} + \frac{w_d}{\rho_p}} \quad (1)$$

where w_w is the weight of the wet membrane (g), w_d is the weight of the dry membrane (g), ρ_e is the density of water and ρ_p is the density of PSf.

The average pore radius (m), r_m can be calculated using the Guerout-Elford–Ferry equation of the pore flow model (Equation 2):[5]

$$r_m = \sqrt{\frac{(2.9 - 1.75\varepsilon)8\eta l Q}{\varepsilon \times A \times \Delta P}} \quad (2)$$

where η is the pure water viscosity (8.9×10^{-4} Pa s), ΔP is the trans-membrane pressure (Pa), l is the membrane thickness (m) and Q is the permeate volume of water per unit of time (m^3/s).

2.4 Membrane Performance

The performance of the synthesised membranes was evaluated using a dead-end stainless steel filtration setup, as shown in Figure 1. Membranes with an effective area of 25 cm^2, 250 mL of water and 100 mg/L ACT solution were used at a transmembrane pressure of 1 bar and filtration time of 2 h, respectively.[13] The membrane was first pre-pressurised at 5 bar for 30 min using distilled water to achieve steady-state operation before continuing with the water flux measurement.[14] The feed was then replaced with the ACT solution to establish the ACT flux and rejection percentage of the membranes. The permeate was collected and concentrations of the ACT in the feed and permeate were measured at a wavelength of 254 nm using a UV-Vis spectrometer (GENESYS 20).[15]

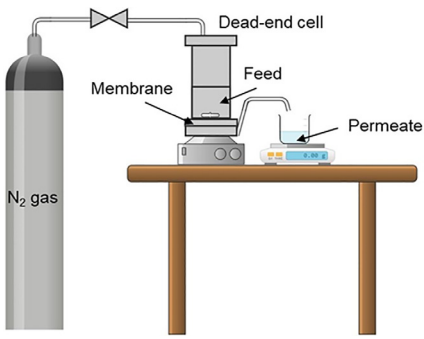

Figure 1: Schematic representation of the membrane filtration setup.

The water and ACT fluxes (F_W, F_{ACT}) were calculated using Equation 3:[16]

$$F = \frac{V}{A\Delta t} \tag{3}$$

where V, F, A and Δt are the permeate volume (L), membrane flux (L/m^2h^1), membrane effective area (m^2) and the filtration time (h), respectively. The rejection, R of the membranes can be calculated using Equation 4:[16]

$$R = \left(1 - \frac{C_p}{C_f}\right) \times 100\% \tag{4}$$

where R, C_p and C_f are the solute rejection (%), and concentration of ACT in the permeate and the feed, respectively.

3. RESULTS AND DISCUSSION

3.1 TiO_2/PSf Membrane Characterisations

3.1.1 Surface and cross-sectional morphologies of the membranes

The addition of hydrophilic particles such as TiO_2 were often proposed since these often results in structure modification that can enhance separation performance. The SEM images of the synthesised TiO_2/PSf membranes are presented in Figure 2. Similar morphologies were observed for all membranes; an asymmetric structure with a thin skin layer with no surface pores and a porous substructure comprising of both the finger-like pores and macrovoids. Moreover, the number of large pores increases with increasing TiO_2 concentration (see Figure 2[A, B, C and D]) but decreases when 2 wt.% of TiO_2 was added to the membrane solution (see Figure 2[E]). This might be associated with the controlling factors during the phase separation. The pore formation was controlled by the thermodynamics and the kinetics of the phase separation process. In terms of thermodynamics, hydrophilic TiO_2 would accelerate the exchange rate between NMP and water, facilitating the formation of greater number of pores structures. Kinetically, the introduction of TiO_2 particles would elevate the viscosity, resulting in slow exchange rate, inhibiting the formation of pore structure.[17]

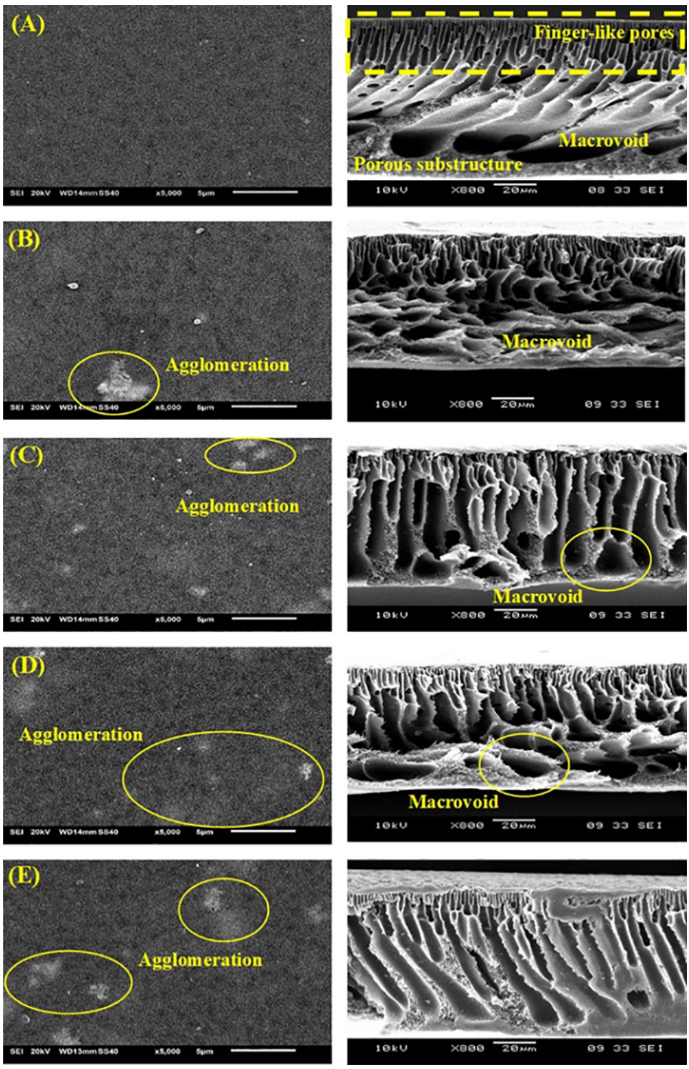

Figure 2: Surface and cross-sectional SEM images of TiO_2/PSf membranes with various TiO_2 concentrations (0 wt.%–2 wt.%): (A) Ti-0.0, (B) Ti-0.5, (C) Ti-1.0, (D) Ti-1.5 and (E) Ti-2.0.

The substructure's finger-like pores have a greater propensity to transform into macrovoids at the addition of TiO_2 at low concentrations, and the macrovoids' length has extended across the membrane thickness, indicating the presence of the thermodynamics effect. The formation of macrovoids was closely related with the solvent and nonsolvent miscibility, as previously reported by Lai et al.[18] When a highly miscible solvent/nonsolvent combination such as NMP/water was used, this can promote the formation of macrovoids. Formation of this structure

typically follows the instantaneous demixing at the nonsolvent/membrane solution interface, producing two phases; the polymer-rich phase at the surface and the polymer-deficient phase at the bottom of the membrane. The diffusion rates of the solvent and nonsolvent were accelerated at the nonsolvent/membrane interface. NMP continuously diffuses into the coagulation bath while water enters the cast membrane, resulting in significant water uptake and high membrane swelling. The rapid merge of PSf occurred at the membrane solution/water interface (polymer-rich region) as a result of PSf/water incompatibility and strong solvent/nonsolvent diffusion, forming a skin layer. Not only that, the hydrophilic TiO_2 nanoparticles also tend to move towards the top layer of the membrane, forming a thicker skin layer.[19] These then hinder the continuous nonsolvent inflow to the membrane solution below this skin layer, subsequently slowing down the exchange between the solvent and nonsolvent inside the membrane substructure. The growth of the polymer in this polymer-deficient phase was delayed, resulting in a looser and larger pore (macrovoids) structure.[20]

Membrane with higher TiO_2 concentration (Ti-2.0) however, showed a similar asymmetric structure but with fewer macrovoids and uniformly built finger-like pores and spongy substructure, suggesting a void-suppressing factor was at play and the transition from porous to spongy structure. At higher TiO_2 concentrations, the viscosity of the dope solution drastically increased due to its larger specific area and surface energy.[19,21] This led to a slower solvent/non-solvent exchange rate, causing a delayed demixing.[22] Additionally, polyvinylpyrrolidone (PVP), which acts as the pore former tends to migrate out during phase inversion.[23] This resulted in a deficiency of pore former, supressing the formation of macrovoids and leading to the production of a finger-like and spongy substructure.[21,24]

Based on the images of the membrane surfaces, white residues were observed on the surface of the membranes with TiO_2, suggesting the occurrence of TiO_2 agglomeration and it increases with increasing TiO_2 concentration from 0.5 wt.%–2.0 wt.%. This phenomenon can be advantageous because this can increase the hydrophilicity of the membrane surface but at the expense of pore blocking. It is believed that significant agglomeration was observed when the attractive intermolecular forces between TiO_2 molecules dominate. This can happen when the surface charge of TiO_2 is nearly zero, in which, the Van der Waals attractive forces are dominant, resulting in increased attractive forces between the TiO_2 molecules and they tend to agglomerate. The agglomerates reduce the effective surface area and therefore, negating the hydroxyl groups on the PSF surface during the demixing process, inhibiting the uniform dispersion of TiO_2 in the membrane. These results are in good agreement with previous reports by Sotto et al. and Vatanpour et al.[25,26]

3.1.2 FTIR analysis

The functional groups of the synthesised TiO_2/PSf membranes were evaluated using FTIR as shown in Figure 3. FTIR spectra show similar prominent peaks at 2,970 cm^{-1}, 1,689 cm^{-1}, 1,585 cm^{-1} and 1,240 cm^{-1}, verifying the presence of PSf as the polymer backbone. This is consistence with the results reported by Kusworo et al. for their PSf-TiO_2/GO membranes.[8,17] The characteristic peaks observed at 1,240 cm^{-1} and 1,585 cm^{-1} confirmed the existence of the O=S=O stretching and the stretching band of C=C aromatic of the PSf polymer, respectively.[27] A weak peak at 2,970 cm^{-1} shows the presence of the C-H group in all membranes although at a very low intensity. A new peak at 690 cm^{-1} was observed for membranes with TiO_2 except for the neat membrane (Ti-0.0), which can be attributed to the presence of TiO_2 inside the membrane. This intense peak can be ascribed to the Ti-O stretching band which is the characteristic peak of TiO_2.[28,29] Not only that, the broad peak at 3,398 cm^{-1}, indicating the presence of the -OH stretching present in Ti-0.0 diminishes with the increasing concentration of the TiO_2 in the membrane.[30] Since TiO_2 nanoparticles have also been reported to have similar peaks attributed to the OH stretching, it was believed that these hydroxyls in both TiO_2 and PSf lead to the formation of the hydrogen bridge bonds, due to the Van Der Waals interaction between the OH groups of TiO_2 and the hydroxyl group of the PSf membrane during the membrane synthesis.[31] The presence of TiO_2, which contains the hydroxyl groups, has also been reported to enhance the hydrophilicity of a membrane, thereby improving water flux.[32]

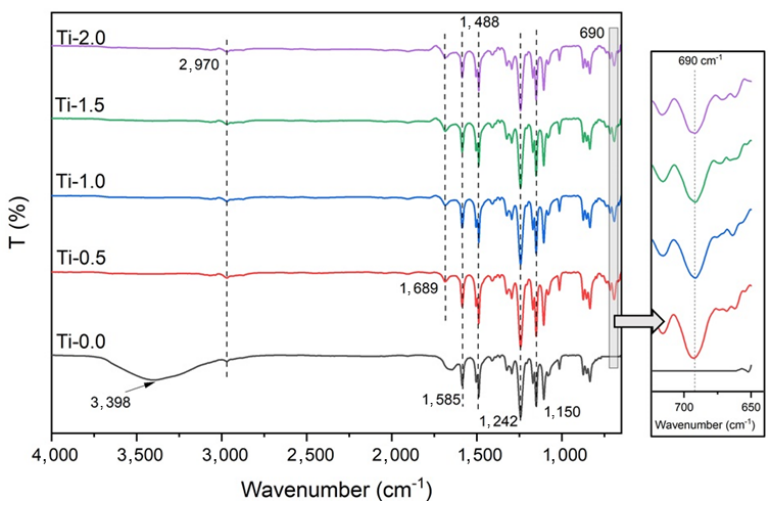

Figure 3: FTIR spectra of TiO_2/PSf membranes with various TiO_2 concentrations (0 wt.%–2 wt.%).

3.1.3 Porosity and average pore size estimation

The membrane thickness, porosity and r_m for all membranes are presented in Table 2. Increased membrane porosity was observed with increasing TiO_2 concentration with the neat PSf membrane (Ti-0.0) recorded the lowest porosity of 74.62%. A noteworthy increase in porosity was recorded for Ti-2.0 membrane and this can be corroborated by the SEM images (see Figure 2[E]) where Ti-2.0 membrane shows a thicker porous substructure as compared to those of the neat PSf membrane (Ti-0.0). These findings can be explained in terms of hydrophilicity of the TiO_2 and the increase of structural vacancies or macrovoids in the polymer structure. As the concentration of hydrophilic TiO_2 increases, it increases the presence of the hydrophilic particles inside the PSf structure, accelerating the exchange rate between the solvent and non-solvent promoting the formation of macrovoids.[33] The formation of larger structural vacancies also increases, subsequently increasing the porosity.

Table 2: Porosity and average pore diameter of fabricated membranes.

Membrane	Thickness (μm)	Porosity (%)	Average pore size, r_m (μm)
Ti-0.0	81	74.62 ± 1.22	16.37
Ti-0.5	68	75.67 ± 0.68	13.15
Ti-1.0	72	76.78 ± 2.45	11.68
Ti-1.5	65	77.16 ± 6.79	10.05
Ti-2.0	73	84.70 ± 1.18	9.79

On the contrary, the average pore size radius, r_m of the synthesised TiO_2/PSf membranes decreases from 16.37 nm–9.79 nm when adding TiO_2 up to 2.0 wt.% (Ti-2.0). This result disagrees with those reported by Yang et al., whereby the porosities of their fabricated PSf with TiO_2 were found to be directly proportional with the pore size.[34] As porosity increases, more space is occupied by pores, allowing for larger pores to form within the membrane structure. However, the variation of surface topography and the size of the aggregated particles on the surface and through the finger-like pores could also affect the size of the pores.[35] At higher TiO_2 concentrations, it is possible that the presence of TiO_2 particles on the membrane surface and inside the pores could potentially blocked the pores partially, decreasing the average pore size.[32] The structural parameters such as porosity and thickness severely affect the transport of water.

3.2 Filtration Performance of TiO_2/PSf Membrane for ACT Removal

The performance of these TiO_2/PSf membranes was evaluated using a filtration system at a low transmembrane pressure of 1 bar. The membrane performance in terms of water flux, ACT flux and rejection is illustrated in Figure 4. The data revealed that the membrane with 2.0 wt.% TiO_2 (Ti-2.0) offered the highest rejection towards ACT and a larger water flux of around 32 L/m^{2}h, which was 25% higher than that of the neat PSf membrane (Ti-0.0). This can be ascribed to an increment in porosity (see Table 2), which promotes the flow of water through the membranes. Even though the average pore size decreases and this usually deteriorates the permeability in many cases, the presence of the hydrophilic TiO_2 particles favourably promotes the transport of more water molecules, boosting the water flux of the membranes.

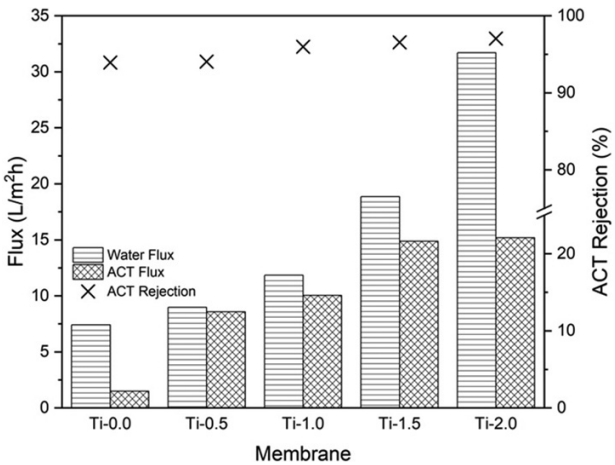

Figure 4: Pure water flux, ACT flux and ACT rejection for TiO_2/PSf membranes with various TiO_2 concentrations (0 wt.%–2 wt.%).

The observed ACT flux showed increment with increasing TiO_2 concentrations, with neat PSF membrane (Ti-0.0) recording the lowest ACT flux of 7.41 L/m^{2}h, attributed to the larger pore size. The larger pore size of the Ti-0.0 membrane resulted in fast filtration as the solution passed through the pores rapidly, reducing the time for the membrane to interact with the ACT molecules.[36] Since Ti-0.0 membrane was synthesised solely from semi-hydrophobic polysulfone with low surface charge, it is more prone to fouling leading to low ACT flux.[37] The average pore size of the membrane decreases due to the introduction of the hydrophilic TiO_2 nanoparticles, subsequently promoting the removal of ACT. However, at 2.0 wt.% TiO_2, no significant increase in flux was observed as compared to the membrane with 1.5 wt.% TiO_2 (Ti-1.5). This is expected since at higher

concentrations, most of the TiO_2 particles agglomerates (see Figure 2), reducing the number of active sites for ACT to interact and can also result in pore blocking, subsequently hindering the ACT removal.[8]

The water flux and ACT rejection of the synthesised membranes were compared (see Table 3) with other commercial polymeric membranes and membranes modified with additives such as methylcellulose (MC) and powdered activated carbon (PAC) under similar membrane filtration conditions as this work. The water flux recorded by Ti-2.0 was comparable to those PSf membranes with MC and PAC but at a higher rejection rate of ACT removal (97%) at low pressure of 1 bar. The reported results of this work revealed the potential of adding TiO_2 into the PSf membrane matrix to remove ACT in membrane technology, although a method to reduce the agglomeration of TiO_2 particles should be considered in the future as this can further elevate the performance of the membrane.

Table 3: Comparison between the performance of TiO_2/PSf membrane with previous research for the removal of ACT.

Membrane	Pollutant	Filtration parameter	Water flux (L/m^2h)	Rejection rate (%)	Ref.
Commercial NF10, NF50	ACT	0.5 L, P = 8 bar, Ci = 100 ppm, pH = 3,6–7, 12	N/A	pH3 = ~38% pH6–7 = ~30% pH12 = ~28%	19
PSf-MC/ PAC	ACT	P = 1 bar, Ci = 100 ppm	39.85	23.15%	5
PES/GO-PA Thin film composite	ACT	P = 1–3, 5 bar, Ci = 10 ppm–20 ppm	~35.00	pH7 = 97.70% pH4 = 29.75%	21
TiO_2/PSf	ACT	P = 1 bar, Ci = 100 ppm	31.707	97%	Present work

4. CONCLUSION

TiO_2/PSf flat sheet membranes were successfully synthesised. The FTIR confirms the successful incorporation of the TiO_2 into the PSf membrane matrix. The performances of the membranes were evaluated in terms of water flux, ACT flux and ACT rejection percentage from aqueous solution containing 100 ppm ACT. The membrane with the highest TiO_2 concentration recorded the best ACT rejection and water flux of 97% and 32 L/m^2h, respectively. This was attributed to its improved morphologies, which provides greater porosity (84.70%) and longer interaction times for ACT and TiO_2 particles. At lower concentrations, TiO_2 particles have successfully modified the membrane morphologies and characteristics to significantly improve the water flux and

rejection rate of ACT. Limitations such as TiO_2 agglomerates observed on the membrane surface which resulted in the lower ACT flux obtained should be prevented. Better methods or surfactants for incorporating TiO_2 into the PSf membrane need to be explored.

5. ACKNOWLEDGEMENTS

The authors would like to acknowledge the support from the Centre of Excellence of Biomass Utilization (CoEBU), Universiti Malaysia Perlis (UniMAP) for assisting in sample preparation throughout this work.

6. REFERENCES

1. Shipingana, L. N. N., Shivaraju, H. P. & Yashas, S. R. (2022). Quantitative assessment of pharmaceutical drugs in a municipal wastewater and overview of associated risks. *Appl. Water Sci*, 12, 16. https://doi.org/10.1007/s13201-022-01570-1
2. Serpone, N. et al. (2017). Light-driven advanced oxidation processes in the disposal of emerging pharmaceutical contaminants in aqueous media: A brief review. *Curr Opin Green Sustain Chem*, 6, 18–33. https://doi.org/10.1016/j.cogsc.2017.05.003
3. Serbanescu, O. S., Voicu, S. I. & Thakur, V. K. (2020). Polysulfone functionalized membranes: Properties and challenges. *Mater. Today Chem.*, 17, 100302. https://doi.org/10.1016/j.mtchem.2020.100302
4. Kheirieh, S., Asghari, M. & Afsari, M. (2018). Application and modification of polysulfone membranes. *Rev. Chem. Eng.*, 34, 657–693. https://doi.org/10.1515/revce-2017-0011
5. Nadour, M., Boukraa, F. & Benaboura, A. (2019). Removal of diclofenac, paracetamol and metronidazole using a carbon-polymeric membrane. *J. Environ. Chem. Eng.*, 7(3), 103080. https://doi.org/10.1016/j.jece.2019.103080
6. Zhang, J. et al. (2015). Enhanced antifouling behaviours of polyvinylidene fluoride membrane modified through blending with nano-TiO_2/polyethylene glycol mixture. *Appl. Surf. Sci.*, 345, 418–427. https://doi.org/10.1016/j.apsusc.2015.03.193
7. Zhang, H. et al. (2020). Preparation and characterization of PSF-TiO_2 hybrid hollow fiber UF membrane by sol–gel method. *J. Polym. Res.*, 27, 376. https://doi.org/10.1007/s10965-020-02313-z
8. Kusworo, T. D. et al. (2021). Preparation and characterization of photocatalytic PSf-TiO_2/GO nanohybrid membrane for the degradation of organic contaminants in natural rubber wastewater. *J. Environ. Chem. Eng.*, 9, 105066. https://doi.org/10.1016/j.jece.2021.105066
9. Razmjou, A., Mansouri, J. & Chen, V. (2011). The effects of mechanical and chemical modification of TiO_2 nanoparticles on the surface chemistry, structure and fouling performance of PES ultrafiltration membranes. *J. Memb. Sci.*, 378, 73–84. https://doi.org/10.1016/j.memsci.2010.10.019

10. Li, J.-F. et al. (2009). Effect of TiO_2 nanoparticles on the surface morphology and performance of microporous PES membrane. *Appl. Surf. Sci.*, 255, 4725–4732. https://doi.org/10.1016/j.apsusc.2008.07.139
11. Wan Ramli, W. K. et al. (2022). Phase separation behaviour modification using co-solvents on PVDF membranes for water filtration. *AIP Conf Proc*, 2541, 040012. https://doi.org/10.1063/5.0113799
12. Wan Ramli, W. K. et al. (2024). Fe_3O_4-Doped polysulfone membrane for enhanced adsorption of copper from aqueous solution. *Malays. J. Anal. Sci.*, 28, 423–440.
13. Nourmoradi, H. et al. (2018). Removal of acetaminophen and ibuprofen from aqueous solutions by activated carbon derived from Quercus Brantii (Oak) acorn as a low-cost biosorbent. *J Environ Chem Eng*, 6(6), 6807–6815. https://doi .org/10.1016/j.jece.2018.10.047
14. Bahri, S. S. et al. (2019). The influence of Fe doped TiO_2 as inorganic additive on the properties of polysulfone ultrafitration membrane. *Malays. J. Fundam. Appl. Sci.*, 15(5), 725–730.
15. Mujahid, A. et al. (2014). Rapid assay of the comparative degradation of acetaminophen in binary and ternary combinations. *Arab. J. Chem.*, 7(4), 522–524. https://doi.org/10.1016/j.arabjc.2012.10.014
16. Zaulkiflee, N. D. et al. (2019). Juxtaposition of Polyethersulfone Composite Membranes: Performance and Antifouling Capability. *J. Phys. Sci.*, 30(Supp. 2), 13–22. https://doi.org/10.21315/jps2019.30.s2.2
17. Liu, X. et al. (2024). A green, efficient, and degradable poly(butylene succinate) (PBS)/TiO_2 hybrid membrane for water treatment. *J. Water Process Eng.*, 61, 105302. https://doi.org/10.1016/j.jwpe.2024.105302
18. Lai, J.-Y. et al. (1999). On the formation of macrovoids in PMMA membranes. *J. Memb. Sci*., 155(1), 31–43. https://doi.org/10.1016/S0376-7388(98)00292-0
19. Safarpour, M., Vatanpour, V. & Khataee, A. (2016). Preparation and characterization of graphene oxide/TiO_2 blended PES nanofiltration membrane with improved antifouling and separation performance. *Desalination*, 393, 65–78. https://doi.org/10.1016/j.desal.2015.07.003
20. Wu, H. et al. (2022). Fabrication of polysulfone membrane with sponge-like structure by using different non-woven fabrics. *Sep. Purif. Technol.*, 297, 121553. https://doi.org/10.1016/j.seppur.2022.121553
21. Hołda, A. K. & Vankelecom, I. F. J. (2015). Understanding and guiding the phase inversion process for synthesis of solvent resistant nanofiltration membranes. *J. Appl. Polym. Sci.*, 132(27). https://doi.org/10.1002/app.42130
22. Sugu, L. & Jawad, Z. A. (2019). Formation of low acetyl content cellulose acetate membrane for CO_2/N_2 separation. *J. Phys. Sci.*, 30, 111–125. https://doi .org/10.21315/jps2019.30.1.9
23. Ho, C.-C. & Su, J. F. (2022). Boosting permeation and separation characteristics of polyethersulfone ultrafiltration membranes by structure modification via dual-PVP pore formers. *Polymer*, 241, 124560. https://doi.org/10.1016/ j.polymer.2022.124560
24. Abdulkarem, E. et al. (2020). Development of Polyethersulfone/α-Zirconium phosphate (PES/α-ZrP) flat-sheet nanocomposite ultrafiltration membranes. *Chem. Eng. Res. Des.*, 161, 206–217. https://doi.org/10.1016/j.cherd.2020.07.006

25. Sotto, A. et al. (2011). Effect of nanoparticle aggregation at low concentrations of TiO_2 on the hydrophilicity, morphology, and fouling resistance of PES–TiO_2 membranes. *J. Colloid. Interface Sci.*, 363(2), 540–550. https://doi.org/10.1016/j.jcis.2011.07.089
26. Vatanpour, V. et al. (2012). TiO_2 embedded mixed matrix PES nanocomposite membranes: Influence of different sizes and types of nanoparticles on antifouling and performance. *Desalination*, 292, 19–29. https://doi.org/10.1016/j.desal.2012.02.006
27. Jiang, Y. et al. (2019). Graphene oxides as nanofillers in polysulfone ultrafiltration membranes: Shape matters. *J. Memb. Sci.*, 581, 453–461. https://doi.org/10.1016/j.memsci.2019.03.056
28. Sun, F. et al. (2021). Dopamine-decorated lotus leaf-like PVDF/TiO_2 membrane with underwater superoleophobic for highly efficient oil-water separation. *Process Saf. Environ. Prot.*, 147, 788–797. https://doi.org/10.1016/j.psep.2021.01.006
29. Al-Amin, M. et al. (2016). Solar assisted photocatalytic degradation of reactive azo dyes in presence of anatase titanium dioxide. *Int. J. Latest Res. Eng. Technol.*, 2(3), 14–21.
30. Sarihan, A. (2020). Development of high-permeable PSf/PANI-PAMPSA composite membranes with superior rejection performance. *Mater. Today Commun.*, 24, 101104. https://doi.org/10.1016/j.mtcomm.2020.101104
31. Wu, C. Y. et al. (2017). Markedly enhanced surface hydroxyl groups of TiO_2 nanoparticles with superior water-dispersibility for photocatalysis. *Materials*, 10(5), 566. https://doi.org/10.3390/ma10050566
32. Li, W. et al. (2013). Preparation and characterization of poly (vinylidene fluoride)/TiO_2 hybrid membranes. *Front Environ. Sci. Eng.*, 7, 492–502. https://doi.org/10.1007/s11783-012-0407-x
33. Chai, P. V. et al. (2017). Evaluation of iron oxide decorated on graphene oxide (Fe_3O_4/GO) nanohybrid incorporated in PSf membrane at different molar ratios for congo red rejection. *J. Teknol.*, 79(1–2). https://doi.org/10.11113/jt.v79.10440
34. Yang, Y. et al. (2007). The influence of nano-sized TiO_2 fillers on the morphologies and properties of PSF UF membrane. *J. Memb. Sci.*, 288(1–2), 231–238. https://doi.org/10.1016/j.memsci.2006.11.019
35. Yuliwati, E. et al. (2011). Characterization of surface-modified porous PVDF hollow fibers for refinery wastewater treatment using microscopic observation. *Desalination*, 283, 206–213. https://doi.org/10.1016/j.desal.2011.02.037
36. Maryam, B. et al. (2020). A study on behavior, interaction and rejection of Paracetamol, Diclofenac and Ibuprofen (PhACs) from wastewater by nanofiltration membranes. *Environ. Technol. Innov.*, 18, 100641. https://doi.org/10.1016/j.eti.2020.100641
37. Garcia-Ivars, J. et al. (2017). Nanofiltration as tertiary treatment method for removing trace pharmaceutically active compounds in wastewater from wastewater treatment plants. *Water Res.*, 125, 360–373. https://doi.org/10.1016/j.watres.2017.08.070